

CRACKED SOILS BEHAVIOR DUE TO DRYING CONDITIONS USING A FUZZY C-MEANS METHOD

*Yerry Kahaditu Firmansyah¹, *Ria Asih Aryani Soemitro², Dwa Desa Warnana³, and Januarti Jaya Ekaputri⁴

^{1,2,4}Civil Engineering Departement, Institut Teknologi Sepuluh Nopember, Indonesia; ³Geophysical Engineering Departement, Institut Teknologi Sepuluh Nopember, Indonesia

**Corresponding Author, Received: 25 July 2019, Revised: 03 Oct. 2019, Accepted: 26 Nov. 2019

ABSTRACT: The drying cycle can affect embankments based on their physical properties and induce soil cracks. This paper investigates the unsaturated physical behavior of material from flood embankments located at the Bengawan Solo River, Pelangwot village, Bojonegoro, East Java, Indonesia. The volumetric shrinkage and degree of compactedness of the soil are important factors that control the soil behavior due to dry conditions. Some tests were conducted to study the desiccation process, in which soil samples were placed in a circular desiccation plate with soil thickness of 10 mm and a 100 mm plate diameter. A water retention curve was obtained to analyze the material properties during shrinkage. Next, the effect of the drying process on geometric characteristics of crack patterns was analyzed by image processing. Then, photo records of cracked soil from laboratory tests were assessed to determine the soil crack intensity via a Fuzzy C-Means (FCM) method using MATLAB software. The image analysis results show that the geometric characteristics of crack patterns were influenced by the drying process with a decrease in water content at 10% intervals until the air-dried condition was achieved. This is consistent with field observations; this indicates that image processing can be used quantitatively to analyze the drying process dependency of soil cracking behavior.

Keywords: Crack evolution, Drying condition, River embankment, Volumetric shrinkage

1. INTRODUCTION

One of the main problems in riverine areas is embankment failure. These failures can be predicted from current river effect conditions and climate changes [1]. Many failures result from soils saturated during the rainy season and unsaturated during the dry season [2]. Several studies have been performed to investigate the drying cycle and how it affects soil physical properties and the mechanical characteristics of soil (e.g., change the moisture content, shear strength, negative water pressure, and volume changes) [2-4].

The volumetric shrinkage and compactedness of soil is an important physical and mechanical parameter that controls the behavior of soil properties in drying conditions [5-8]. The effect of the drying process on the geometric characteristics of crack patterns was analyzed by image processing [5,9,10]. These studies indicate that image processing can be used quantitatively to analyze the drying process dependence of cracking behavior [9].

Photographs of cracked soil generated from laboratory tests can be assessed to determine of cracking intensity with Fuzzy c-means numerical modeling. FCM clustering is a technique that has been successfully applied to feature analysis,

clustering, and classifier designs in fields such as astronomy, geology, medical imaging, target recognition, and image segmentation [11-15]. This study was conducted to observe cracked soil particularly to index the CIF (Crack Intensity Factor) on the soil by using the FCM method.

The FCM method has a very high degree of accuracy, but the resolution of the picture must be clear. Furthermore, the geometric characteristics of surface crack patterns are described and quantified through image processing, and the mechanisms involved are discussed.

2. MATERIALS AND METHODS

The soil investigation was located at a section of embankment along Bengawan Solo River at Pelangwot village, in the region of Bojonegoro, Indonesia (Fig. 1). The samples were obtained at depths from 0.3 m to 0.5 m from the surface with disturbed and undisturbed conditions. The soil was classified as an inorganic silt of high compressibility [6]. Some basic properties of the soil are listed in Table 1. The chemical composition using X-Ray Fluorescence method of the soil is shown in Table 2; it was found that the soil chemical compounds are mainly silica (Si) and Calcium (Ca). The minerals of the clay fraction

play a central role in the properties of the soil, such as plasticity and strength [6].

Table 1. Properties of Bengawan Solo soil

Properties	Value (%)
Liquid limit	135.0
Plastic limit	100.8
Plasticity index	34.2
Linear shrinkage	9.9
Volumetric shrinkage	12.55
Particle Size Distribution (PSD)	
Sand	4.54
Silt	44.98
Clay	50.48

Table 2. The chemical composition of Bengawan Solo river embankment soil

Element	by weight (%)
Al	8.7
Si	28.3
K	1.5
Ca	22.6
Ti	2.18
V	0.099
Mn	0.878
Fe	34.6
Cu	0.2
Zn	0.079
Sr	0.39
Zr	0.2
Ba	0.3
Re	0.07

2.1 Compaction Test

The as built constructed river embankment is Proctor compacted. The soil specimen was prepared as Proctor compacted. It was essential to investigate the compaction behavior of the river embankment Bengawan Solo, as the soils were to be remolded and compacted for laboratory tests, and the results of the compaction test a guide to remolded crack soil sample. The standard test methods for laboratory compaction using characteristics of soil using standard effort were carried out according to The American Society for Testing Materials (ASTM) D698, with input energies per unit volume of 12,400 ft-lbf/ft³. A maximum dry density of 1.43 gr/cm³ at an optimum moisture content of 27% was determined for the standard Proctor dry density conditions (Fig. 2). The man-made sections of embankments were constructed at 80–85% of the optimum standard Proctor dry density during the dry season, with the fill material at moisture contents drier than optimum [17].

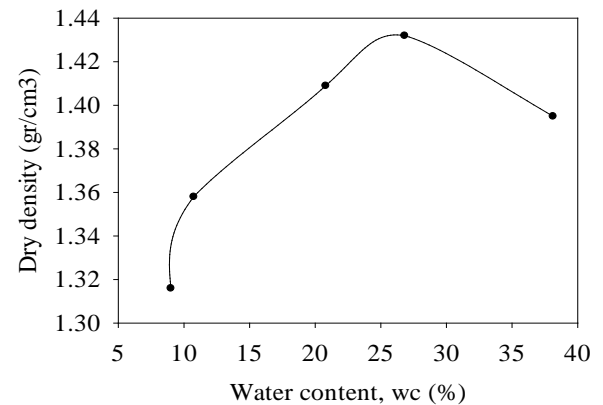


Fig 2. Compaction curve with initial soil conditions

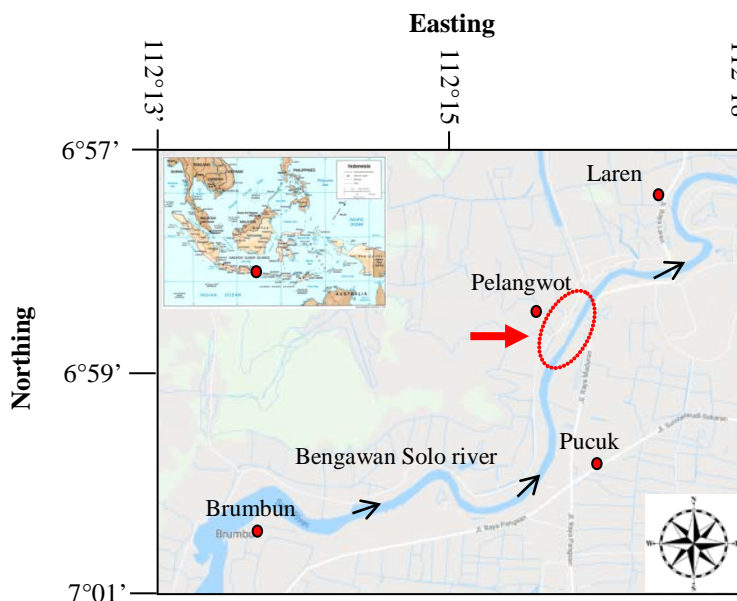


Fig 1. Study location

2.2 Shrinkage Test

The shrinkage characteristics of the soil were most important to this study. The specimen for the volumetric shrinkage test was prepared according to ASTM D 427 – 04. In a well-ventilated room, the specimen was air-dried slowly to avoid the formation of shrinkage cracks. From the shrinkage curve in Fig. 3, the shrinkage limit for river embankment Bengawan Solo was found to be 12.55%.

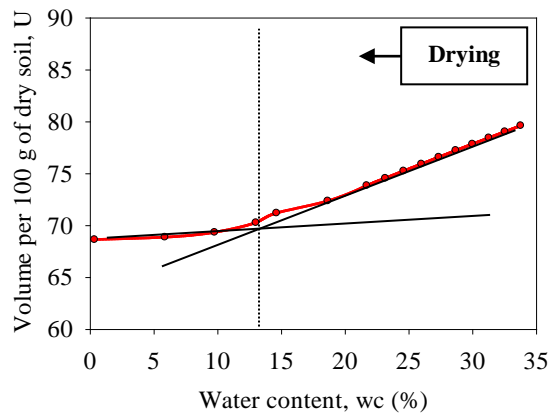


Fig 3. Shrinkage curve for river embankment Bengawan Solo (section from Pelangwot village)

Other research has shown that the shrinkage limit for Bengawan Solo Soil was found to be 16.45% [5]. The characteristic soil properties and effort used for compaction were very influential towards the value of the shrinkage limit.

2.3 Desiccation Test

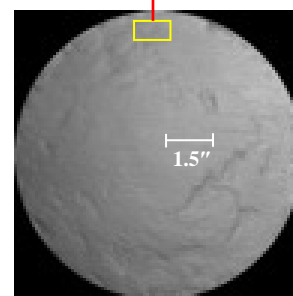
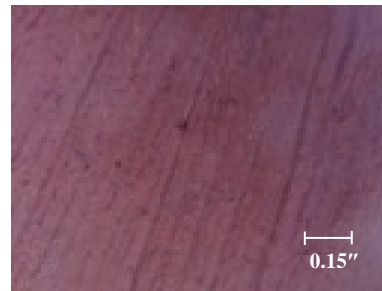
To study desiccation behavior, first, the soil was air-dried and sieved through a 4.75 mm sieve, and the soil specimen was remolded on a circular plate with 10 mm soil thickness and 100 mm surface diameter (Fig. 4). The sieved soil was mixed with water to achieve optimum moisture content and soil density concerning the compaction test. The sample has been prepared manually placing soil into the molds. The sample has been measured and recorded the weight of the specimen with water content decreasing at 10% intervals until air-dried conditions were achieved.



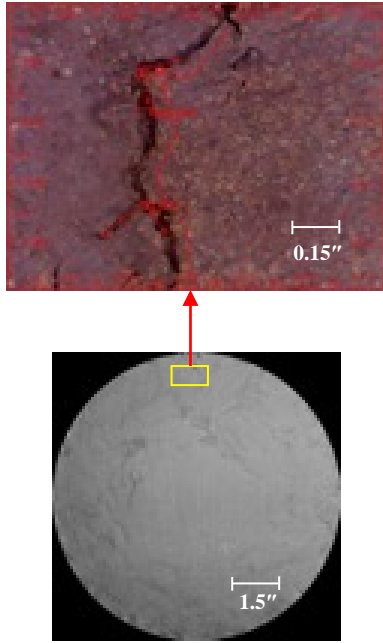
Fig 4. Soil specimen was remolded on a circular plate with 10 mm soil thickness and 100 mm surface diameter.

2.4 Record of Cracks by Digital Imaging

Digital imaging was performed on the specimens at a macro and micro scale. Example macro and micro photos are shown in Fig. 5. Cracked soil does not occur at the beginning of the drying process (Fig. 5a). However, initial cracked soil occurs when the water content decreases at the first interval during the drying process (Fig. 5b).



a. Water content (Wc) of a specimen is 33.7%



b. Specimen Wc is 32.5%

Fig 5. Images of soil specimen with decreasing water content

2.5 FCM Clustering

The FCM algorithm assigns pixels to each category by using fuzzy memberships. Let $X = (x_1, x_2, \dots, x_N)$ denotes an image with N pixels to be partitioned into c clusters, where x_i represents multispectral (features) data [23]. The algorithm is an iterative optimization that minimizes the cost function defined as follows:

$$J = \sum_{j=1}^N \sum_{i=1}^c u_{ij}^m \|x_j - v_i\| \quad (1)$$

where u_{ij} represents the membership of pixel x_j in the i th cluster, v_i is the i th cluster center, $\|\cdot\|$ is a norm metric, and m is a constant. The parameter m controls the fuzziness of the resulting partition, and $m = 2$ is used in this study.

The cost function is minimized when pixels close to the centroid of their clusters are assigned high membership values, and low membership values are assigned to pixels with data far from the centroid. The membership function represents the probability that a pixel belongs to a specific cluster. In the FCM algorithm, the probability is dependent solely on the distance between the pixel and each individual cluster center in the feature domain [23]. The membership functions and cluster centers are updated by the following:

$$u_{ij} = \frac{1}{\sum_{k=1}^c \left(\frac{\|x_j - v_i\|}{\|x_j - v_k\|} \right)^{2/(m-1)}}, \quad (2)$$

and

$$v_i = \frac{\sum_{j=1}^N u_{ij}^m x_j}{\sum_{j=1}^N u_{ij}^m}. \quad (3)$$

Starting with an initial guess for each cluster center, the FCM converges to a solution for v_i representing the local minimum or a saddle point of the cost function. Convergence can be detected by comparing the changes in the membership function or the cluster center at two successive iteration steps.

2.6 Spatial FCM

One of the important characteristics of an image is that neighboring pixels are highly correlated. In other words, these neighboring pixels possess similar feature values, and the probability that they belong to the same cluster is great [23]. This spatial relationship is important in clustering, but it is not utilized in a standard FCM algorithm. To exploit the spatial information, a spatial function is defined as

$$h_{ij} = \sum_{k \in NB(x_j)} u_{ik}, \quad (4)$$

where $NB(x_j)$ represents a square window centered on pixel x_j in the spatial domain. A 5×5 window was used throughout this work. Just like the membership function, the spatial function h_{ij} represents the probability that pixel x_j belongs to i th cluster. The spatial function of a pixel for a cluster is large if the majority of its neighborhood belongs to the same clusters. The spatial function is incorporated into membership function as follows:

$$u'_{ij} = \frac{u_{ij}^p h_{ij}^q}{\sum_{k=1}^c u_{kj}^p h_{kj}^q} \quad (5)$$

where p and q are parameters to control the relative importance of both functions. In a homogenous region, the spatial functions simply fortify the original membership, and the clustering result remains unchanged. However, for a noisy pixel, this formula reduces the weighting of a

noisy cluster by the labels of its neighboring pixels. As a result, misclassified pixels from noisy regions or spurious blobs can easily be corrected. The spatial FCM with parameter p and q is denoted $sFCM_{p,q}$. Note that $sFCM_{1,0}$ is identical to the conventional FCM.

The clustering is a two-pass process at each iteration. The first pass is the same as that in standard FCM to calculate the membership function in the spectral domain. In the second pass, the membership information of each pixel is mapped to the spatial domain, and the spatial function is computed from that. The FCM iteration proceeds with the new membership that is incorporated with the spatial function. The iteration is stopped when the maximum difference between two cluster centers at two successive iterations is less than a threshold ($= 0.02$). After the convergence, defuzzification is applied to assign each pixel to a specific cluster for which the membership is maximal.

2.7. Cluster Validity Functions

Two types of cluster validity functions, fuzzy partition and feature structure, are often used to evaluate the performance of clustering in different clustering methods. The representative functions for the fuzzy partition are partition coefficient V_{pc} [19] and partition entropy V_{pe} [20]. They are defined as follows:

$$V_{pc} = \frac{\sum_j^N \sum_i^c u_{ij}^2}{N} \quad (6)$$

and

$$V_{pe} = \frac{-\sum_j^N \sum_i^c [u_{ij} \log u_{ij}]}{N} \quad (7)$$

The idea of these validity functions is that the partition with less fuzziness means better performance. As a result, the best clustering is achieved when the value V_{pc} is maximal or V_{pe} is minimal.

The disadvantages of V_{pe} and V_{pc} are that they measure only the fuzzy partition and lack a direct connection to the featuring property. Other validity functions based on the feature structure are available [21,22]. For example, Xie and Beni [21] defined the validity function as

$$V_{xb} = \frac{-\sum_j^N \sum_i^c u_{ij} \|x_j - v_i\|^2}{N * (\min_{i \neq k} \{\|v_k - v_i\|^2\})} \quad (8)$$

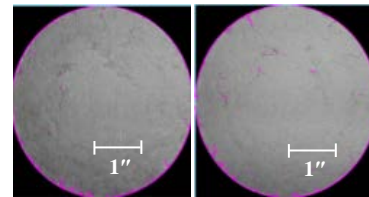
A good clustering result generates samples that are compacted within one cluster and samples that are separated between different clusters. Minimizing V_{xb} is expected to lead to a good clustering.

2.8 Quantitative Analysis of Crack Intensity with FCM Numerical Modelling

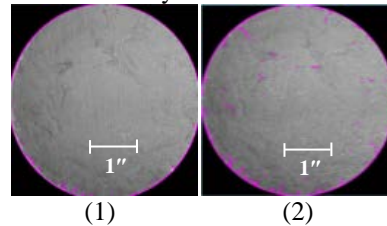
The FCM method was used to analyze the digital images for crack evolution and deformation. As for the visual analysis to investigate the crack soil using the MATLAB software-based FCM method.

An image can be represented in various feature spaces, and the FCM algorithm is classifies the image by grouping similar data points in the feature space into clusters. This clustering is achieved by iteratively minimizing a cost function that is dependent on the distance of the pixels to the cluster centers in the feature domain. A custom application of this technique is CIS (crack identification of soil).

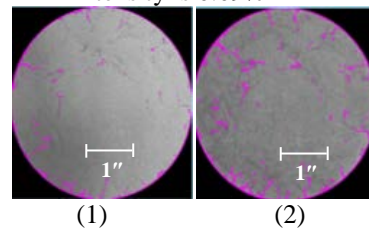
CIS software has been designed to characterize and quantify soil cracks. The result was calculated and analyzed with MATLAB software using the FCM method as shown in Fig. 6.



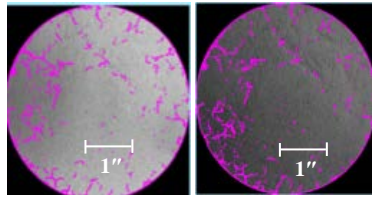
a. Specimen for (1) Wc is 32.5% and crack intensity is 0.03%; (2) Wc is 31.2% and crack intensity is 0.04%



b. Specimen for (1) Wc is 29.9% and crack intensity is 0.07%; (2) Wc is 28.6% and crack intensity is 0.09%

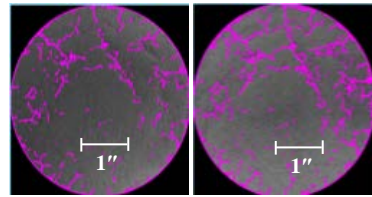


c. Specimen for (1) Wc is 27.3% and crack intensity is 0.10%; (2) Wc is 25.9% and crack intensity is 0.14%



(1) (2)

d. Specimen for (1) Wc is 24.5% and crack intensity is 0.46%; (2) Wc is 23.1% and crack intensity is 0.61%



(1) (2)

e. Specimen for (1) Wc is 21.6% and crack intensity is 0.73%; (2) Wc is 18.6% and crack intensity is 1.16%

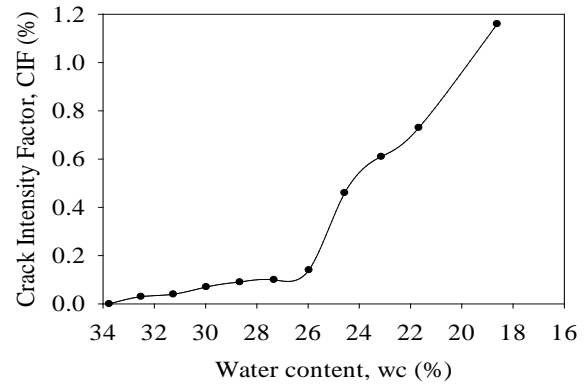
Fig 6. Crack analysis with MATLAB software-based fuzzy c-means (FCM) method

3. RESULT AND DISCUSSION

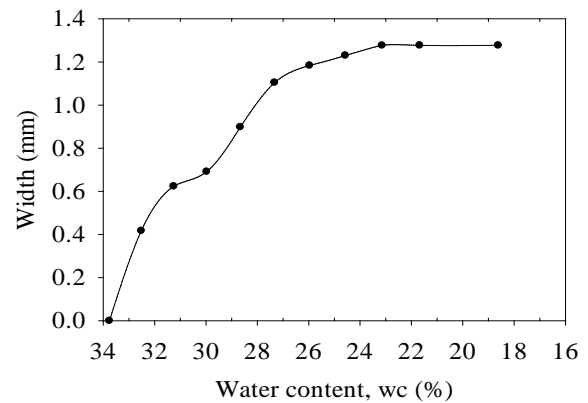
It is commonly thought that desiccating clay soils crack when the tensile stress developed in the soil due to the matric soil suction exceeds the tensile strength of the soil [18].

Information on the evolution of cracked soil (e.g., crack intensity factor, average width, rate of crack, drying process temperature, and time duration) is shown in Fig. 7. A ruler on a microscope program determined the total length of crack. The crack intensity is the ratio of the surface area of the cracks to the total surface area of the soil.

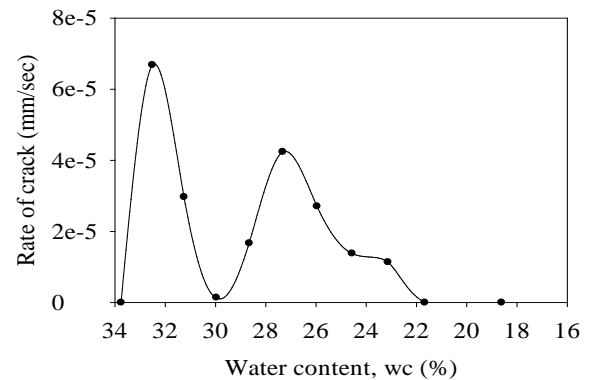
The most significant change phase in the Crack Intensity Factor (CIF) in the soil when a water content (wc) is 26% (Fig. 7a) but the width of the cracks on the soil tends to be constant (Fig. 7b). The rate of the crack is very influenced by temperature (Fig. 7c), experiments conducted on specimens are made as in real conditions on river embankments. The temperature drops during at night (Fig. 7d) and need more time to become wide cracked (Fig. 7e).



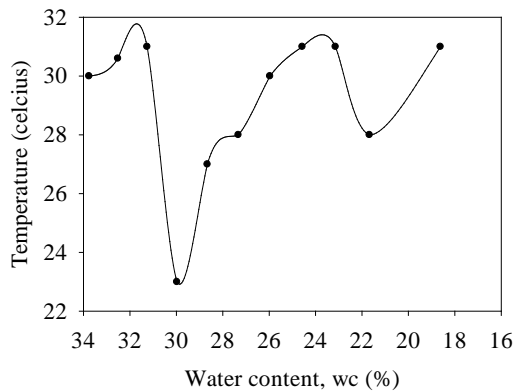
(a). Crack intensity during the drying process



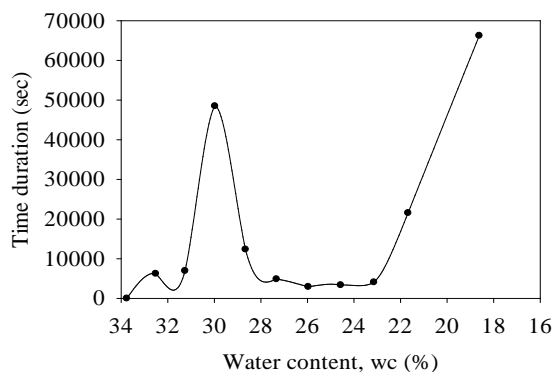
(b). The width of crack during the drying process



(c). The rate of crack during the drying process



(d). The temperature of crack during the drying process



(e). The time duration of cracks during the drying process

Fig 7. Changes in properties of cracked soil during the drying process

The properties of the cracked soil are strongly affected by temperature and time factors. The drying process increased the crack intensity soil width of cracked soil but not always linearly; after a certain soil desiccation level, soil crack intensity did not decrease.

4. CONCLUSIONS

This work focuses on the study of some relevant factors that affect the behavior of soils during the drying process. Desiccation and cracking behavior of soil layers taken from a slurry state, compacted and remolded and subjected to a drying process were investigated through laboratory experiments. The process of surface crack evolution, structural evolution and volume shrinkage behavior were monitored. The following conclusions can be drawn:

- a. The identification and calculation of cracked soils using Fuzzy C-Means (FCM) were successful.
- b. Cracked soils occurred during the first step drying process.
- c. The crack intensity increased with an average value of 0.12%
- d. The maximum width of cracks was 1.27 mm.

5. ACKNOWLEDGMENTS

We would like to thank *Pendidikan Magister Doktor Sarjana Unggul (PMDSU)* program from Indonesian Ministry of Research and Higher Education for the scholarship and research grant.

6. REFERENCES

- [1] Shoqib (2014) News Report at Desa Serenan, Kecamatan Juwiring. Solo pos Newspaper.
- [2] Goh SG, Rahardjo H, Leong EC, and Asce M (2014) Shear Strength of Unsaturated Soils Under Multiple Drying-Wetting Cycles. ASCE – Journal of Geotechnical and Geoenvironmental Engineering Pp 140.
- [3] Nalendro N, and Azis (2006) Effect of Wetting and Drying Soil Infiltration In Solo River Embankment. Final Project, Institut Teknologi Sepuluh Nopember (in Indonesian).
- [4] Colina H, and Roux S (2000) Experimental model of cracking induced by drying shrinkage. The European Physical Journal 1: 189-194.
- [5] Atique A, and Sanchez M (2011) Analysis of Cracking Behavior of Drying Soil. 2nd International Conference on Environmental Science and Technology IPCBEE, IACSIT Press, Singapore, vol 6.
- [6] McCloskey G, Sanchez M, and Soemitro RAA (2008) Experimental behavior of compacted silt used in a flood defense embankment in Indonesia. Proceedings of International Conference on Geotechnical & Highway Engineering, Kuala Lumpur, Malaysia, (ISBN: 978-983-42613-4-4): 26-27.
- [7] Sun DA, Sheng DC, Cui HB, and Li J (2006) Effect of Density on The Soil water-Retention Behavior of Compacted Soil. ASCE- Unsaturated Soils.
- [8] Mountassir GE, Sanchez M, Romer E, and Soemitro RAA (2010) Behavior of Compacted Silt Used To Construct Flood Embankment. Proceedings of The Institution of Civil Engineers, Geotechnical Engineering, Doi: 10.1680/Geng.10.00055.
- [9] Tang CS, Cui YJ, Shi B., Tang AM, and Liu C (2011) Desiccation and Cracking Behavior of Clay Layer From Slurry State Under Wetting–Drying Cycles. Elsevier-Geoderma 166: 111–118.

- [10] Laras LL (2015) Assessment To Soil Properties Associated With Desiccation Crack of Natural and Metakaolin Based Geopolymer Stabilized Soil. Dissertation, Institut Teknologi Sepuluh Nopember.
- [11] Yan A, Wu K, and Zhang X (2002) A quantitative study on the surface crack pattern of concrete with high content of street fiber. *Cem. Concr. Res* 32: 1371-1375.
- [12] Bezdek J, Hall L, and Clarke L (1993) Review of MR image segmentation using pattern recognition. *Med Phys* 20:1033–1048.
- [13] Lye NS, Kandel A, and Schneider M (2002) Feature-based fuzzy classification for interpretation of mammograms. *Fuzzy Sets Syst* 114:271–280.
- [14] Chuang KS, Tzeng HL, Chen S, Wu J, and Chen TJ (2006) Fuzzy C-Means Clustering with Spatial Information for Image Segmentation. *Elsevier - Computerized Medical Imaging and Graphics* 30: 9– 15.
- [15] Pham DL, Xu C, and Prince JL (2000) Current Methods in Medical Image Segmentation. *Annual Review of Biomedical Engineering* 2: 315 – 337.
- [16] Yang MS, Hu YJ, Lin KCR, and Lin CCL (2002) Segmentation techniques for tissue differentiation in MRI of Ophthalmology using fuzzy clustering algorithms. *Magn Reson Imaging* 20:173–179.
- [17] Soemitro RAA, Leong EC, Rahardjo H, and Choa V (1997) Application of Soil water Characteristic Curve To Vacuum Preloading. *Geotechnical Engineering in Asia: 2000 and Beyond, Third Asian Young Geotechnical Engineers Conference, Singapore, 14 – 16 May 1997, Pp. 221-230.*
- [18] Kodikara JK, and Thusyanthan NI (2008) Modelling of desiccation crack development in clay soils. The 12th International conference of International Association for Computers Methods and Advances in Geomechanics (IACMAG) Goa, India, 1-6 October 2008:
- [19] Bezdek JC. Cluster validity with fuzzy sets. *J Cybern* 1974;3:58–73.
- [20] Bezdek JC. Mathematical models for systematic and taxonomy. In: proceedings of eighth international conference on numerical taxonomy, San Francisco; 1975, p. 143–66.
- [21] Xie XL, Beni GA. Validity measure for fuzzy clustering. *IEEE Trans Pattern Anal Mach Intell* 1991;3:841–6.
- [22] Fukuyama Y, Sugeno M. A new method of choosing the number of clusters for the fuzzy c-means method. In: proceedings of fifth fuzzy system symposium; 1989, p. 247–50.
- [23] Keh-Shih Chuang, Et Al 2006. “Fuzzy C-Means Clustering with Spatial Information for Image Segmentation” *Elsevier-Computerized Medical Imaging and Graphics* 30 (2006) 9– 15

Copyright © Int. J. of GEOMATE. All rights reserved, including the making of copies unless permission is obtained from the copyright proprietors.
